Resonant Feshbach scattering of fermions in one-dimensional optical lattices

J. Phys. B: At. Mol. Opt. Phys. **40** (2007) 2703–2718 doi:10.1088/0953-4075/40/13/014

Resonant Feshbach scattering of fermions in one-dimensional optical lattices

M Grupp[1], R Walser[1], W P Schleich[1], A Muramatsu[2] and M Weitz[3]

[1] Institut für Quantenphysik, Universität Ulm, Albert-Einstein-Allee 11, D-89081 Ulm, Germany
[2] Institut für Theoretische Physik III, Universität Stuttgart, Pfaffenwaldring 57, D-70550 Stuttgart, Germany
[3] Institut für Angewandte Physik der Universität Bonn, Wegelerstraße 8, D-53115 Bonn, Germany

E-mail: michael.grupp@uni-ulm.de

Received 10 May 2007, in final form 17 May 2007
Published 20 June 2007
Online at stacks.iop.org/JPhysB/40/2703

Abstract

We consider Feshbach scattering of fermions in a one-dimensional optical lattice. By formulating the scattering theory in the crystal momentum basis, one can exploit the lattice symmetry and factorize the scattering problem in terms of centre-of-mass and relative momentum in the reduced Brillouin zone scheme. Within a single-band approximation, we can tune the position of a Feshbach resonance with the centre-of-mass momentum due to the non-parabolic form of the energy band.

(Some figures in this article are in colour only in the electronic version)

1. Introduction

It is well known from solid state theory [1, 2], x-ray defraction [3] or the atomic motion in laser fields [4] that the presence of a periodic potential requires a modification of the conventional concepts of scattering theory [5]. In the context of ultra-cold quantum gases, this has led to a tremendous outburst of activities during the past few years. Today, it is possible to examine the interplay of many-body physics at the lowest attainable temperature, in the presence of designable optical lattices [6] for bosons [7–10], fermions [11–14], bose–fermi mixtures [15, 16] and to manipulate simultaneously the interaction among particles [17–21], as well as collective states [22].

In the present paper, we will discuss binary Feshbach resonance scattering in the presence of a lattice, as a particular aspect of the aforementioned general theme. When one approaches the topic of binary atomic scattering in homogeneous space and in a periodic lattice, one needs to highlight the similarities and differences, first. In homogeneous space the scattering process connects asymptotical free states, which are plane waves $|q\rangle$. The accessible relative kinetic energy $q^2 > 0$ forms a simple continuum, which has a lower bound, but no upper

one. Furthermore, a binary scattering event in homogeneous space is translational invariant. As a consequence, one obtains the separation of the centre-of-mass motion from the relative dynamics, hence a significant simplification of the problem. In optical lattices in contrast, we have to use the eigenstates of a lattice, i.e. Bloch states $|q, n\rangle$ with a quasi-momentum q and band-index n. Due to the periodic potential, we find a structured energy continuum $\epsilon_L(q, n)$, which consists of several bands n of increasing width (defining upper and lower band edges), as well as forbidden gaps. The density of states also varies accordingly.

The discrete translational symmetry of the lattice can be exploited for the scattering problem by introducing a crystal momentum basis [23], which is formed by two-particle free Bloch states $|q_1, n_1\rangle \otimes |q_2, n_2\rangle$. They are labelled by the centre-of-mass momentum $Q = q_1 + q_2$ modulo the crystal momentum k_L, which remains a good quantum number. In this way, the coupled two-particle scattering simplifies again and we can introduce a scattering amplitude to measure the strength of the binary interaction.

By introducing the Feshbach coupling, in addition to the normal pairing potential between two fermions, we will be able to enhance the strength of binary interactions via an external magnetic field [24]. Being in a lattice, we can consider interband interactions in addition to the intraband transitions. This will be important if the strength of the Feshbach coupling is comparable to the interband separation. For simplicity, we will consider here only very narrow resonances, such that a single-band description is sufficient. Extensions to multi-band configurations are straightforward in the present formulation, if necessary [25].

In this paper, we present the principle of a scattering calculation for two fermions in a one-dimensional lattice. In section 2, we will start from the current form of the many-body theory that is pursued by many groups. We will simplify this by considering only two fermions and a compound bosonic molecule to obtain a two-component two-particle Schrödinger equation for the molecule and fermion-pair wavefunction. In section 3, we will briefly review the basic concept of the scattering phase, the transmission probability and discuss the simplest model for a Feshbach resonance in homogeneous space. This will be generalized to two-particle Feshbach scattering in a one-dimensional lattice in section 4. We present numerical results for Feshbach resonance within a single-band approximation and demonstrate that it can be tuned selectively with the centre-of-mass momentum, due to the non-parabolic energy band.

2. Reducing many-body physics to two atoms and a molecule

Currently, much effort is devoted to the many-body description of resonance superfluidity and the BEC–BCS crossover [26–28]. Thus, we will briefly introduce the fundamental model Hamiltonian [29, 30]. Then, we will apply it to the situation of only two fermions and a bosonic molecule, now, trapped in the same periodic one-dimensional optical lattices. The periodic trapping of both molecular and atomic components is beneficial to the overall interaction cross section as both components will tend to be localized at the anti-nodes of the optical potential, thus be constantly available for scattering.

In the language of second quantization, we describe the many-body system with fermionic fields $\hat{\psi}_\sigma(\boldsymbol{x})$, which remove a single-fermionic particle from position $\boldsymbol{x}$ in internal state $\sigma = \{\uparrow, \downarrow\}$, and molecular bosonic fields $\hat{\phi}_i(\boldsymbol{x})$, which annihilate a composite bound two-particle excitation from the centre-of-mass space-point $\boldsymbol{x}$ in internal configuration i. These field operators and their adjoints satisfy the usual fermionic anti-commutation rules

$$\left\{\hat{\psi}_{\sigma_1}(\boldsymbol{x}_1), \hat{\psi}^\dagger_{\sigma_2}(\boldsymbol{x}_2)\right\} = \delta(\boldsymbol{x}_1 - \boldsymbol{x}_2)\delta_{\sigma_1\sigma_2}, \qquad \left\{\hat{\psi}_{\sigma_1}(\boldsymbol{x}_1), \hat{\psi}_{\sigma_2}(\boldsymbol{x}_2)\right\} = 0, \quad (1)$$

and bosonic commutation rules

$$\left[\hat{\phi}_{i_1}(\boldsymbol{x}_1), \hat{\phi}^\dagger_{i_2}(\boldsymbol{x}_2)\right] = \delta(\boldsymbol{x}_1 - \boldsymbol{x}_2)\delta_{i_1 i_2}, \qquad \left[\hat{\phi}_{i_1}(\boldsymbol{x}_1), \hat{\phi}_{i_2}(\boldsymbol{x}_2)\right] = 0, \quad (2)$$

respectively. We want to consider only bound molecular excitations by choosing a high dissociation threshold energy. Effectively this closes this decay channel and allows only for collision-induced processes. These are the basic ingredients of a Feshbach resonance as originally invented by Fermi, Fano and Feshbach [31–33]. Hence, we can present the composite molecular field also with respect to the individual coordinates $(\mathbf{x}_1, \mathbf{x}_2)$ of the dimer, i.e.

$$\hat{\phi}(\mathbf{x}_1, \mathbf{x}_2) = \sum_i \hat{\phi}_i((\mathbf{x}_1 + \mathbf{x}_2)/2)\langle \mathbf{x}_2 - \mathbf{x}_1 | i\rangle. \tag{3}$$

The dynamics of the multi-component gas is governed by a total system Hamiltonian

$$\hat{H} = \hat{H}_L + \hat{V} \tag{4}$$

$$\hat{H}_L = \int \mathrm{d}^3x \sum_{\sigma=\{\uparrow,\downarrow\}} \hat{\psi}^\dagger_\sigma(\mathbf{x}) H_L(\mathbf{x}, \mathbf{p}) \hat{\psi}_\sigma(\mathbf{x}) + \int \mathrm{d}^6x\, \hat{\phi}^\dagger(\mathbf{x}_1, \mathbf{x}_2) H_L(\mathbf{x}_1, \mathbf{p}_1, \mathbf{x}_2, \mathbf{p}_2) \hat{\phi}(\mathbf{x}_1, \mathbf{x}_2), \tag{5}$$

$$\begin{aligned}\hat{V} = \int \mathrm{d}^6x \big\{ & v_q(\mathbf{x}_1 - \mathbf{x}_2)\hat{\phi}^\dagger(\mathbf{x}_1, \mathbf{x}_2)\hat{\phi}(\mathbf{x}_1, \mathbf{x}_2) + [g^*(\mathbf{x}_1 - \mathbf{x}_2)\hat{\phi}^\dagger(\mathbf{x}_1, \mathbf{x}_2)\hat{\psi}_\downarrow(\mathbf{x}_2)\hat{\psi}_\uparrow(\mathbf{x}_1) + \mathrm{H.c.}] \\ & + v_p(\mathbf{x}_1 - \mathbf{x}_2)\hat{\psi}^\dagger_\uparrow(\mathbf{x}_1)\hat{\psi}^\dagger_\downarrow(\mathbf{x}_2)\hat{\psi}_\downarrow(\mathbf{x}_2)\hat{\psi}_\uparrow(\mathbf{x}_1)\big\}.\end{aligned} \tag{6}$$

It consists of the lattice Hamiltonian $\hat{H}_L$ and the interactions $\hat{V}$ between atoms and molecules. We assume that the free dynamics of the atoms and molecules is determined by their kinetic and potential energy in a quasi-1d optical lattice

$$H_L(\mathbf{x}, \mathbf{p}) = -\frac{\hbar^2}{2m}\nabla^2 + U_L(x) + U_\perp(y, z), \tag{7}$$

where $\mathbf{x} = (x, y, z)$ and $\mathbf{p} = -\mathrm{i}\hbar\nabla$ are canonically conjugate variables in the position representation, m is the atomic mass and $U_L(x)$ is a one-dimensional optical lattice potential. Furthermore, we want to assume that the motion in the perpendicular (y, z) direction is effectively frozen out by a tight confinement potential $U_\perp(y, z)$. Supposedly, the lattice energy is identical for the fermionic atoms of both kinds and twice that for the molecules, i.e.

$$H_L(\mathbf{x}_1, \mathbf{p}_1, \mathbf{x}_2, \mathbf{p}_2) = H_L(\mathbf{x}_1, \mathbf{p}_1) + H_L(\mathbf{x}_2, \mathbf{p}_2). \tag{8}$$

The binary interaction potential v_p accounts for the non-resonant interaction of 'spin-up' and 'spin-down' fermions, the coupling strength g converts free fermionic particles into bound bosonic molecular excitations and v_q is the molecular potential with at least one bound state. One can further simplify matters by considering only even parity binary interaction potentials v_q, v_p and g. Moreover, we have neglected the interactions among the molecules, since we will focus on the case of just two fermions.

The essence of the resonant scattering physics in this many-body Hamiltonian can be brought out most clearly, if we consider only two interacting fermionic atoms with field amplitude ψ and a bosonic molecule with amplitude ϕ, i.e.

$$|\Psi(t)\rangle = \int \mathrm{d}^6x \big\{\phi(\mathbf{x}_1, \mathbf{x}_2, t)\hat{\phi}^\dagger(\mathbf{x}_1, \mathbf{x}_2) + \psi(\mathbf{x}_1, \mathbf{x}_2, t)\hat{\psi}^\dagger_\uparrow(\mathbf{x}_1)\hat{\psi}^\dagger_\downarrow(\mathbf{x}_2)\big\}|0\rangle. \tag{9}$$

According to the Pauli principle, the bosonic and fermionic part of the total wavefunction must be symmetric and anti-symmetric under particle exchange. Thus, if we limit the discussion to the fermionic singlet channel, we need to have a symmetric spatial amplitude $\psi(\mathbf{x}_1, \mathbf{x}_2, t) = \psi(\mathbf{x}_2, \mathbf{x}_1, t)$, as well as a symmetric molecular wavefunction $\phi(\mathbf{x}_2, \mathbf{x}_1, t) = \phi(\mathbf{x}_1, \mathbf{x}_2, t)$.

In this restricted few-particle Fock space with the imposed constraints on the interaction channels, finally one finds a two-component Schrödinger equation for the state vector $\boldsymbol{\chi}(\mathbf{x}_1, \mathbf{x}_2, t) = (\phi(\mathbf{x}_1, \mathbf{x}_2, t), \psi(\mathbf{x}_1, \mathbf{x}_2, t))^\top$

$$\begin{aligned} \mathrm{i}\hbar\partial_t \boldsymbol{\chi} &= [H_L(\mathbf{x}_1, \mathbf{p}_1, \mathbf{x}_2, \mathbf{p}_2) \otimes \mathbb{1} + V(\mathbf{x}_1 - \mathbf{x}_2)]\,\boldsymbol{\chi}, \\ V(\mathbf{x}) &= \begin{pmatrix} v_q(\mathbf{x}) & g(\mathbf{x}) \\ g^*(\mathbf{x}) & v_p(\mathbf{x}) \end{pmatrix}. \end{aligned} \tag{10}$$

In the following, we will also abandon the three-dimensional character of the problem and restrict the discussion to a quasi one-dimensional situation, when all dynamics takes place along the x-direction.

3. Scattering in free space

The previously introduced two-component Hamiltonian contains the essential ingredients of Feshbach scattering, but lacks the full translational invariance of homogeneous space, due to the presence of the lattice potential. We will therefore briefly review the scattering phase and the prerequisites for the appearance of a Feshbach resonance in free space with a contact potential for later reference.

3.1. Scalar potential scattering

The energy of two particles on a line

$$H = H_0(p_1) + H_0(p_2) + V(x_1 - x_2), \tag{11}$$

consists of kinetic energy $H_0 = p^2/2m$ and the short-range binary potential energy V. Obviously, all parts of this Hamiltonian are translational invariant. This symmetry can be exploited by introducing a centre-of-mass coordinate X and a relative coordinate x, as well as their conjugate momenta P, p as

$$X = (x_1 + x_2)/2, \qquad x = x_1 - x_2, \tag{12}$$

$$P = p_1 + p_2, \qquad p = (p_1 - p_2)/2. \tag{13}$$

The total momentum P is the conserved quantity that is associated with the symmetry generating displacement operator $\mathcal{D}_{12}(a) = \exp[\mathrm{i}aP/\hbar]$. It shifts the whole system by a distance a in the $\mathbf{e}_{12} = \mathbf{e}_1 + \mathbf{e}_2$ direction and commutes with the Hamiltonian

$$[H, \mathcal{D}_{12}(a)] = 0. \tag{14}$$

Thus, the total two-body wavefunction $\chi_2(x_1, x_2)$ can be expressed in terms of centre-of-mass and relative coordinates with a product ansatz $\chi_2(x_1, x_2) = \theta(X)\chi(x)$. Here, we assume that $\theta(X) = \exp(\mathrm{i}QX)$ is a plane wave in the centre-of-mass coordinate with momentum Q and the relative wavefunction is denoted by $\chi(x)$. This reduces the corresponding two-particle Schrödinger equation with total energy E to the standard form [5] of an effective single-particle problem

$$\left[\frac{\mathrm{d}^2}{\mathrm{d}x^2} + \varepsilon - V(x)\right]\chi(x) = 0, \tag{15}$$

where we have also rescaled all dimensional quantities, like length $x \to xk_L$, in terms of the wave-number k_L of an optical lattice photon (see equation (25)), as well as energies or potentials $V \to V/\varepsilon_L$, in terms of the recoil energy $\varepsilon_L = \hbar^2 k_L^2/m$. Adopting such units will

facilitate the comparison with the lattice case discussed in section 4. Then, the relative energy ε becomes synonymous with the free space dispersion relation

$$\varepsilon(k) = k^2 = E - \frac{Q^2}{4} > 0. \tag{16}$$

As any second-order differential equation, equation (15) admits two linearly independent scattering solutions $\chi_k^{(\pm)}(x)$ for the same energy $\varepsilon(k)$. By comparing them to non-interacting plane waves, one can introduce reflection and transmission amplitudes $R(k)$ and $T(k)$, i.e.

$$\begin{aligned}\lim_{x\to-\infty} \chi^{(+)}(x,k) &= \mathrm{e}^{\mathrm{i}kx} + R\,\mathrm{e}^{-\mathrm{i}kx} \\ &= \mathrm{e}^{\mathrm{i}\delta_e}\cos(kx-\delta_e) + \mathrm{i}\,\mathrm{e}^{\mathrm{i}\delta_o}\sin(kx-\delta_o),\end{aligned} \tag{17}$$

$$\begin{aligned}\lim_{x\to\infty} \chi^{(+)}(x,k) &= T\,\mathrm{e}^{\mathrm{i}kx} \\ &= \mathrm{e}^{\mathrm{i}\delta_e}\cos(kx+\delta_e) + \mathrm{i}\,\mathrm{e}^{\mathrm{i}\delta_o}\sin(kx+\delta_o)\end{aligned} \tag{18}$$

as well as even and odd scattering phase shifts $\delta_e(k)$ and $\delta_o(k)$. The transmission and reflection probabilities are given by

$$|T|^2 = \cos^2(\delta_e - \delta_o), \qquad |R|^2 = \sin^2(\delta_e - \delta_o), \tag{19}$$

and unitarity demands current conservation, which is mathematically paraphrased as $|T|^2 + |R|^2 = 1$.

3.2. Two-component Feshbach resonances with a contact potential

The quintessential mechanism for a Feshbach resonance occurs, when one couples two internal states $\boldsymbol{\chi} = (\chi_q, \chi_p)^\top$ to the external motion of the one-dimensional, two-particle Hamiltonian of equation (11). The closed q-channel needs an attractive delta potential to support a bound state and a localized coupling matrix element is required to provide an interaction with the open p-channel [34]. A simple, analytically solvable model for this is

$$\begin{aligned} H &= H_0(p_1, p_2) \otimes \mathbb{1} + V(x_1 - x_2), \\ V(x) &= \begin{pmatrix} u + v\delta(x) & g\delta(x) \\ g\delta(x) & 0 \end{pmatrix}. \end{aligned} \tag{20}$$

The parameters of the potential matrix V are the threshold energy $u > 0$, the strength of the closed channel potential $v < 0$ and the channel coupling parameter g. As in the scalar case, all contributions to the Hamiltonian are translationally invariant and a product ansatz for the wavefunction $\boldsymbol{\chi}_2(x_1, x_2) = \exp(\mathrm{i}QX)\boldsymbol{\chi}(x)$ leads to the Schrödinger equation for the relative wavefunction

$$\left[\frac{\mathrm{d}^2}{\mathrm{d}x^2} + \varepsilon - V(x)\right]\boldsymbol{\chi}(x) = 0. \tag{21}$$

Here, we have again introduced rescaled potentials, energies and length mentioned in the context of equation (15).

For relative scattering energies $0 < \varepsilon(k) = k^2 < u$, smaller than the threshold energy u, the closed channel asymptotic wavefunction $\chi_q(x)$ vanishes exponentially, while the open channel wavefunction $\chi_p(x)$ propagates outwards freely. Due to the even parity of the contact

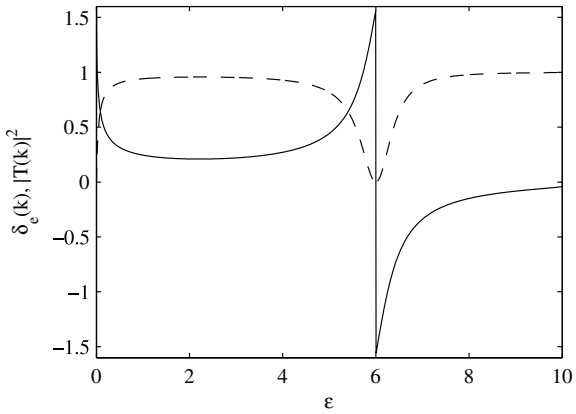

Figure 1. Even scattering phase $\delta_e(k)$ (solid line) and transmission probability $|T|^2$ (dashed line) of a Feshbach resonance as a function of energy $\varepsilon = k^2$ with a resonance at $\varepsilon_{\rm res} = 6$. Parameters: $u = 10$, $v = -4$ and $g = 1$.

potential, we can also choose wavefunctions of definite parity, i.e.

$$\lim_{x\to\pm\infty} \chi_q^{(e)}(x,k) \sim \mathrm{e}^{-q|x|}, \qquad q(k) = \sqrt{u-k^2}, \tag{22}$$

$$\lim_{x\to\pm\infty} \chi_p^{(e)}(x,k) \sim \cos(kx \pm \delta_e). \tag{23}$$

Odd wavefunctions do not accrue any phase shift, as they vanish at the point of interaction.

By integrating the coupled Schrödinger equation (21) over an infinitesimal strip around the discontinuity, one obtains the necessary boundary conditions to compute the scattering phase of the even wavefunction. After some minor algebra, one obtains the phase shifts

$$\tan(\delta_e) = -\frac{g^2}{2k(2q(k)+v)}, \qquad \delta_o = 0. \tag{24}$$

This phase shift and the corresponding transmission probability $|T|^2$ of equation (19) are depicted in figure 1. One clearly observes the Feshbach resonance with a π-phase jump at $\varepsilon_{\rm res} = k_{\rm res}^2 = u - v^2/4$. The position of the resonance energy is usually controlled by changing the dissociation threshold energy u via magnetic fields or via the depth of the bound state potential v, which is a property of the considered atomic element and, thus, harder to modify. The width of the resonance is primarily determined by the coupling strength g [35]. Due to the vanishing odd phase shift, the total reflection $T = 0$ also occurs at the same energy, when the even phase shift reaches $\delta_e(k_{\rm res}) = \pi/2$. It is also important to note that the phase can be well approximated by a Breit–Wigner curve in the vicinity of the resonance.

In figure 2, we present the same scattering phase $\delta_e(k(E, Q))$ of equation (24), now as a function of the two-particle energy E and the centre-of-mass momentum Q, according to (16). This representation emphasizes the parabolic form of the resonance energy $E_{\rm res} = \varepsilon_{\rm res} + Q^2/4 > 0$, as a function of Q. The Feshbach resonance is always present for $\varepsilon_{\rm res} > 0$ and for all Q, or it disappears if $\varepsilon_{\rm res} < 0$. As we will show in the following sections, this fundamental behaviour can be changed by considering Feshbach scattering in a lattice where centre-of-mass and relative motion are coupled. Results can be seen in figures 11 and 12.

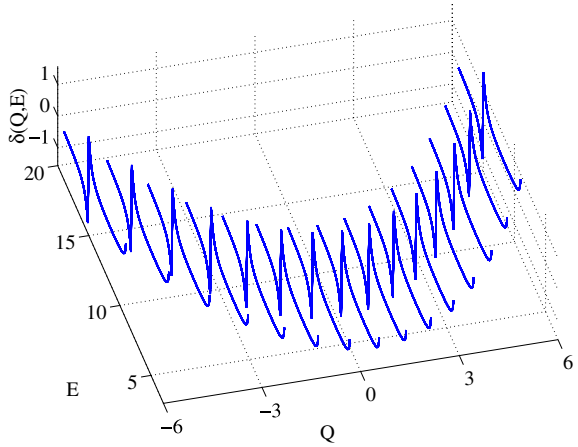

Figure 2. Even scattering phase $\delta_e(k(Q, E))$ versus energy E and momentum Q. The Feshbach resonances are located on a free space parabola as a function of Q. Parameters as in equation (32).

4. Scattering on a one-dimensional lattice

4.1. Bloch states and periodic boundary conditions

Studying physics in periodic structures immediately leads to the consideration of Bloch states [2, 36], which reflect the discrete translation symmetry $\mathcal{D}(la) = \exp[\mathrm{i}lap/\hbar]$ of the Hamiltonian $[H_L, \mathcal{D}(la)] = 0$ with $l \in \mathbb{N}$. We have already introduced a quasi-one-dimensional lattice Hamiltonian in equation (7) and will disregard from now on the transverse degrees of motion, i.e.

$$H_L(x, p) = \frac{p^2}{2m} + U_L(x), \qquad U_L(x) = U_L \cos^2(k_L x/2). \tag{25}$$

The lattice potential $U_L(x + a) = U_L(x)$ is characterized by a lattice constant a, which in turn defines the crystal momentum $k_L = 2\pi/a$. Thus, the eigenstates of the Schrödinger equation

$$H_L|q, n\rangle = \varepsilon_L^n(q)|q, n\rangle, \tag{26}$$

can be classified as Bloch states $|q, n\rangle$ with quasi-momentum $-\pi/a \leqslant q < \pi/a$, and energy bands $\varepsilon_L^n(q)$, labelled by band index n. According to the Bloch theorem

$$\langle x|q, n\rangle = \mathrm{e}^{\mathrm{i}qx} u_q^n(x), \qquad u_q^n(x + a) = u_q^n(x). \tag{27}$$

Such an energy eigenfunction can be decomposed into a plane-wave phase factor and a lattice periodic function u_q^n. Subjected to translation to the next lattice site, the wavefunction acquires a complex phase

$$\langle x + a|q, n\rangle = \mathrm{e}^{\mathrm{i}qa}\langle x|q, n\rangle. \tag{28}$$

The periodic continuation in momentum space has its subtleties and attention needs to be paid to the vanishing of the wavefunction at the centre or edge of the first Brillouin zone [36]. However, the generic case is simply given by $\langle x|q + k_L, n\rangle = \langle x|q, n\rangle$.

In practice, it is usually necessary to work with a discrete subset of Bloch states, which are found by considering a periodically continued, finite lattice with an even number of wells $N = 2M$. The Born–von-Karman periodic boundary conditions then require that

$$\langle x + L|q, n\rangle = \mathrm{e}^{\mathrm{i}qL}\langle x|q, n\rangle = \langle x|q, n\rangle \tag{29}$$

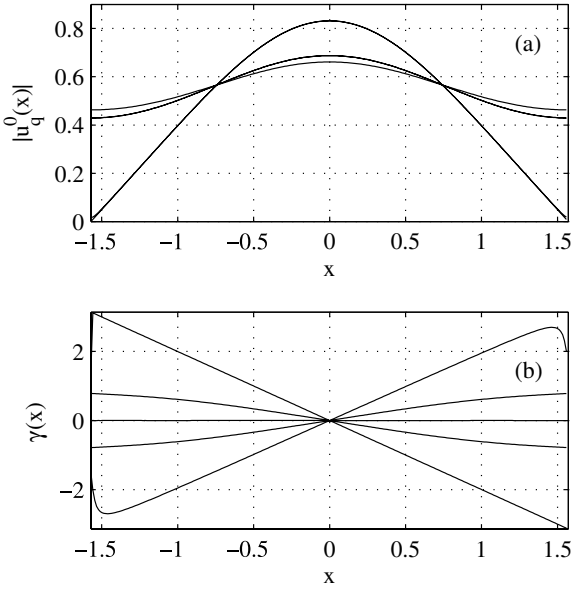

Figure 3. Magnitude $|u_q^0(x)|$ (a) and phase $\gamma(x)$ (b) of the lowest band Bloch function $\langle x|q, n=0\rangle = |u_q^n(x)|\exp[\mathrm{i}\gamma(x)]$, versus dimensionless position $-\pi/2 \leqslant x < \pi/2$, for a few momenta $q = (-1, -0.5, 0, 0.5, 0.992)$. In this shallow potential the Bloch waves are almost plane and deviations are only seen at the band edge $q \approx \pm 1$. Parameters are as in equation (32).

where the total length $L = Na$. This can only be true if there are exactly N distinct momenta q_l in each band

$$-\frac{\pi}{a} \leqslant q_l = \frac{2\pi l}{L} = k_L \frac{l}{N} < \frac{\pi}{a}, \qquad -\frac{N}{2} \leqslant l < \frac{N}{2}. \tag{30}$$

We choose the following orthogonalization for the Bloch states on a finite lattice:

$$\langle q_1, n_1|q_2, n_2\rangle = N\delta_{q_1,q_2}\delta_{n_1,n_2}, \qquad \int_0^a \mathrm{d}x\,|\langle x|q, n\rangle|^2 = 1. \tag{31}$$

The general behaviour of the Bloch states is shown in figure 3. There we have selected a few Bloch eigenfunctions for some momenta q within the Brillouin zone, which exemplify the modified plane-wave behaviour. A typical energy-band structure in coordinate and momentum space is presented in figures 4 and 5, respectively. In here and all of the following calculations, we use dimensionless parameters for a shallow lattice that only supports one band below the barrier, i.e.

$$U_L = -(6/5)^2, \qquad a = \pi, \qquad N = 2^8. \tag{32}$$

4.2. Scalar two-particle scattering in lattices

We will now consider the scattering of two particles in the presence of a lattice. Thus, we have a two-particle lattice Hamiltonian and a binary interaction V

$$H = H_L(x_1, p_1) + H_L(x_2, p_2) + V(x_1 - x_2). \tag{33}$$

By forming two-particle basis states out of single-particle Bloch waves one obtains two-dimensional Bloch states

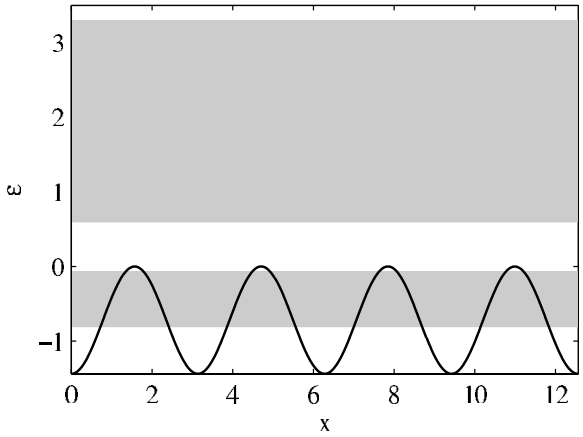

Figure 4. Lattice potential $U_L(x)$ (solid line) versus position x, superimposed on the top of two allowed energy bands $\varepsilon_L^0(q)$ and $\varepsilon_L^1(q)$ (shaded grey). Parameters as in equation (32).

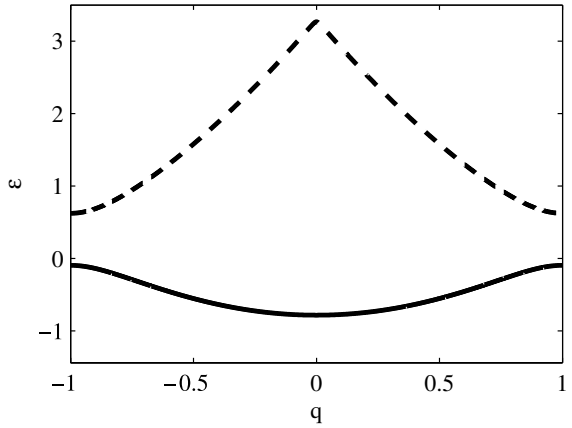

Figure 5. Energy bands $\varepsilon_L^0(q)$ (solid) and $\varepsilon_L^1(q)$ (dashed) versus quasi-momentum q in the first Brillouin zone $-1 \leqslant q < 1$.

$$|Q, q, n_1, n_2\rangle = |q_1(Q, q), n_1\rangle \otimes |q_2(Q, q), n_2\rangle \tag{34}$$

$$Q = q_1 + q_2, \qquad q = (q_1 - q_2)/2 \tag{35}$$

$$q_1 = Q/2 + q, \qquad q_2 = Q/2 - q. \tag{36}$$

The corresponding reciprocal momentum space for two particles in a one-dimensional lattice is depicted in figure 6. One can see the individual single-particle momenta q_1 and q_2, as well as the centre-of-mass momentum Q and relative momentum q. This set of symmetry adjusted basis states can be used to represent a general quantum state with quasi-momentum Q as

$$|\chi, Q\rangle = \sum_{q, n_1, n_2} \chi_Q^{(n_1, n_2)}(q) |Q, q, n_1, n_2\rangle \tag{37}$$

$$\mathcal{D}_{12}(la)|\chi, Q\rangle = \mathrm{e}^{\mathrm{i}laQ}|\chi, Q\rangle. \tag{38}$$

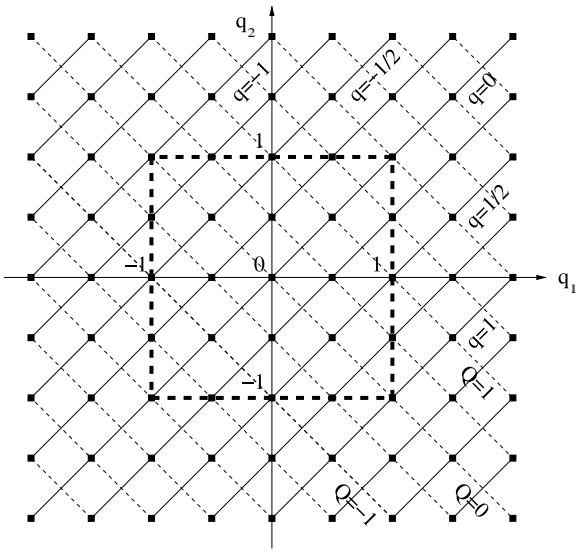

Figure 6. Reciprocal momentum space for two particles in a one-dimensional lattice consisting of only $N = 4$ wells. The Cartesian axes represent the individual momenta in the reduced zone scheme $-1 \leqslant q_1, q_2 < 1$. The 45° rotated grid lines correspond to the contours of centre-of-mass $-1 \leqslant Q < 1$ and relative momentum $-1 \leqslant q < 1$.

From the discrete translation symmetry of the system, one finds the selection rule

$$0 = \langle \chi, Q|[H, \mathcal{D}_{12}(la)]|\chi, Q'\rangle = \langle \chi, Q|H|\chi, Q'\rangle(\mathrm{e}^{\mathrm{i}la(Q'-Q)} - 1), \tag{39}$$

which implies $Q' = Q \bmod k_L$. In the following, we will consider only transitions within the lowest energy band, i.e. $n_1 = n_2 = 0$ and simplify the notation to $\chi_Q^{(0,0)}(q) \equiv \chi_Q(q)$, consequently.

Within these assumptions, one can represent the Schrödinger equation to equation (33) as

$$0 = \sum_{q'} \left\{ \left[\varepsilon_L^0(q_1) + \varepsilon_L^0(q_2) - E \right] \delta_{qq'} + V_Q(q, q') \right\} \chi_Q(q'), \tag{40}$$

where $q_1 = q_1(Q, q)$ and $q_2 = q_2(Q, q)$. If we let our perturbation tend to zero, then we are left with the two-dimensional energy surface

$$E_L(Q, q) = \varepsilon_L^0(q_1) + \varepsilon_L^0(q_2). \tag{41}$$

The contour lines of which are depicted in figure 7. The marked intersections show that there are two linearly independent two-particle quantum states labelled by (q_1, q_2) and (q_2, q_1) that have the same total energy E and centre-of-mass momentum Q. It it interesting to note that in general there are no straight contour lines at $Q = \pm 1$ or $q = \pm 1$, as would be the case in the tight binding limit $|U_L| \gg 1$. The energy range that is covered by the two-particle energy can be seen in figure 8. It shows the projections along the Q and q momentum lines.

Now, if we turn to the evaluation of the matrix element $V_Q(q, q')$, then it is best expressed in centre-of-mass coordinates. Moreover, the algebra simplifies considerably if we use a zero-range contact potential for the binary potential $V(y) = v\delta(y)$ and obtain

$$V(Q, q, q') = v v_Q(q, q'), \tag{42}$$

$$v_Q(q, q') = \int_0^a \frac{\mathrm{d}x}{N} \{ u^*_{Q/2+q}(x) u^*_{Q/2-q}(x) u_{Q/2+q'}(x) u_{Q/2-q'}(x) \}. \tag{43}$$

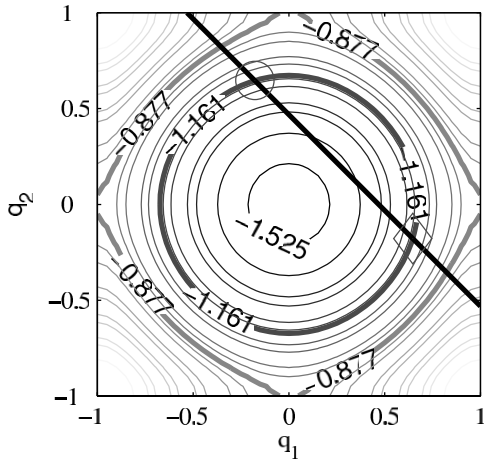

Figure 7. Energy contours $E_L(Q, q)$ for the non-interacting two-particle system in momentum space. The superimposed $Q = \text{const.}$ line (solid black) has two intersections with another $E = \text{const.}$ contour (dark grey), which are at q (circled) and $-q$ (boxed).

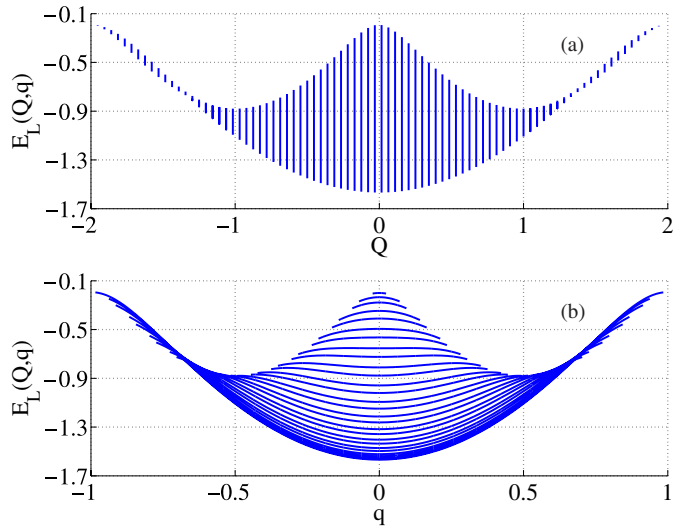

Figure 8. Projections of the two-dimensional energy surface $E_L(Q, q)$ versus momentum Q (a) and q (b).

The shape of this potential matrix can be calculated quite accurately with localized Wannier functions in the Gaussian approximation. In general, this agrees well with the numerical results shown in figure 9. In this picture, we have chosen a value of $Q = 0$ for the centre-of-mass momentum. For other values $Q \neq 0$, one obtains a modest variation of the shape of the matrix element at the momentum edges, but it remains predominantly constant inside.

4.3. Two-component Feshbach scattering in lattices

Having established the basic notions and concepts in the previous sections, we can now turn to the Feshbach resonance scattering phenomenon in a lattice. The basic Hamiltonians have

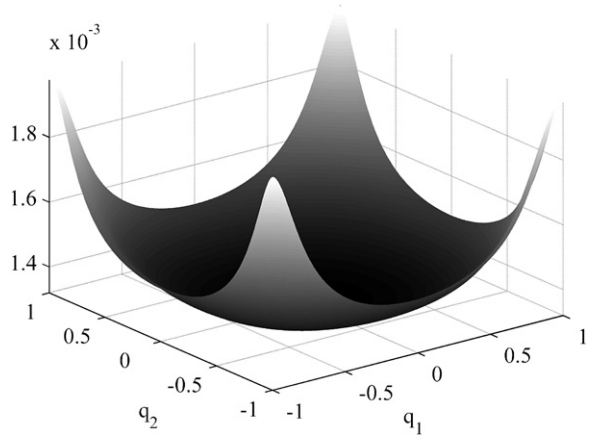

Figure 9. Interaction matrix element $v_Q(q, q')$ in reciprocal momentum space for $Q = 0$, other parameters as in equation (32).

been already introduced in equations (10), (20) and (33). Explicitly, we have the motion in the lattice Hamiltonian H_L, as well as the Feshbach potential V

$$H = H_L(x_1, p_1, x_2, p_2) \otimes \mathbb{1} + V(x_1 - x_2)$$
$$V(x) = \begin{pmatrix} u + v\delta(x) & g\delta(x) \\ g\delta(x) & 0 \end{pmatrix}. \tag{44}$$

Here we have deliberately disregarded the pairing potential $v_p = 0$, as it only provides a modification to the Feshbach phenomenon. The state of the coupled two-component system in the lowest Bloch band $n = 0$ is now defined as

$$|\chi, Q\rangle = \sum_q \begin{pmatrix} \phi_Q(q) \\ \psi_Q(q) \end{pmatrix} |Q, q\rangle, \tag{45}$$

where we have characterized the state with the momentum Q and labelled the open and closed channels by the molecular ϕ and two-fermion wavefunction ψ as in (10).

In order to obtain the Bloch representation of the Schrödinger equation to (44)

$$E|\chi, Q\rangle = H|\chi, Q\rangle, \tag{46}$$

we project it on the two-particle Bloch eigenstate and get

$$E\begin{pmatrix} \phi_Q(q) \\ \psi_Q(q) \end{pmatrix} = \sum_{q'} \left\{ \left[\varepsilon_L^0(q_1(Q, q)) + \varepsilon_L^0(q_2(Q, q))\right]\delta_{qq'} + \delta_{qq'} \begin{pmatrix} u & 0 \\ 0 & 0 \end{pmatrix} + v_Q(q, q') \begin{pmatrix} v & g \\ g & 0 \end{pmatrix} \right\} \begin{pmatrix} \phi_Q(q') \\ \psi_Q(q') \end{pmatrix}. \tag{47}$$

We have numerically diagonalized this Schrödinger equation for the lattice parameters of (32) and the Feshbach parameters $u = 1.5, v = -7, g = 0.03$. Due to the parity of the Hamiltonian, one can sort the resulting $2N$ eigenstates into even and odd states and assign them a positive or negative quantum index $-N \leqslant \nu < N$. By turning off the coupling between the manifolds i.e. $g = 0$, one can distinguish easily the eigenvalues $E_\nu(Q, g = 0)$ that belong to the molecular (q-channel) or the open fermionic spectrum (p-channel). We have depicted a few representative values in (figure 10(a)). It can be seen clearly that there is a single bound state embedded in the allowed energy band of the open p-channel. In figure 10(b), we present

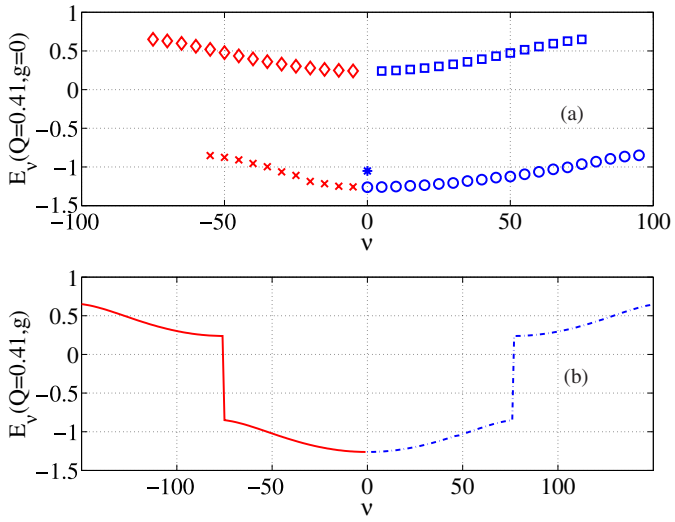

Figure 10. Discrete eigenenergies $E_\nu(Q, g)$ versus quantum number $-N \leqslant \nu < N$ for momentum $Q = 0.41$. Negative quantum numbers label odd states, while positive numbers count even states. (a) Energies of uncoupled system $E_\nu(Q, g = 0)$. Note the location of the bound state ($*$) of the molecular manifold ($\diamondsuit$, $\square$) is inside the fermionic spectrum marked by ($\times$, $\circ$). (b) All interacting eigenenergies $E_\nu(Q, g = 0.03)$ versus quantum index ν. Odd states (solid) and even states (dashed dotted). The bound state is now an admixture of molecular and fermionic manifolds.

the interacting eigenvalues $E_\nu(Q, g = 0.03)$, which are now formed by admixtures of both manifolds and can only be distinguished by the parity of the state.

In order to describe the scattering resonance, we use the standing wave version of the Lippmann–Schwinger equation [5]

$$|\chi^{(s)}, Q, q\rangle = \mathbf{e}_p \otimes |Q, q\rangle + G_L^{(s)}(E)V|\chi^{(s)}, Q, q\rangle, \tag{48}$$

where $\mathbf{e}_p \otimes |Q, q\rangle$ represents a non-interacting Bloch wave in the asymptotically open p-channel $\mathbf{e}_p = (0, 1)^\top$. For the lattice Hamiltonian H_L, one obtains a standing wave Green's function $G_L^{(s)}$ from the usual retarded and advanced Green's functions $G_L^{(\pm)}$ by

$$G_L^{(s)}(E) = \tfrac{1}{2}\big(G_L^{(+)}(E) + G_L^{(-)}(E)\big), \tag{49}$$

$$G_L^{(\pm)}(E) = \lim_{\epsilon \to 0+} \frac{1}{E \pm \mathrm{i}\epsilon - H_L}. \tag{50}$$

Finally, the effect of scattering is measured by the off-shell Heitler- or K-matrix element

$$K_Q(q', q) = \langle Q, q'|\mathbf{e}_p^\top V|\chi^{(s)}, Q, q\rangle. \tag{51}$$

We assign an even on-energy shell scattering phase shift

$$\tan[\delta_e(Q, E)] = K_Q(q, q'), \qquad E = E(Q, q) = E(Q, q'). \tag{52}$$

We have evaluated this phase shift for two differently strong bound molecular states and varied the centre-of-mass momentum of the two-particle collision. In figure 11, one can see the Feshbach resonance cutting into the energy band and disappearing once it is outside. This is modified in figure 12, which has a lesser bound resonance, and therefore does not leave at the lower band edge.

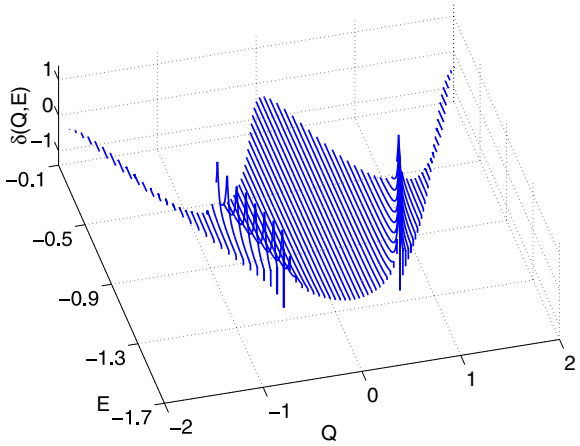

Figure 11. Even scattering phase shift $\delta_e(E, Q)$ of a two-particle Bloch wave versus energy E and momentum Q. One can see clearly Feshbach resonances symmetrically located around the Q-axis, which disappears when the bound state is outside the band. Parameters: $u = 1.5$, $v = -7$, $g = 0.03$.

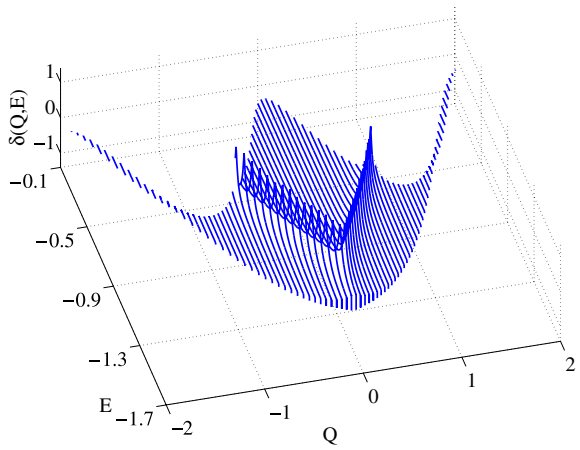

Figure 12. Even scattering phase shift $\delta_e(E, Q)$ of a two-particle Bloch wave versus energy E and momentum Q. With a less deeply bound state the resonances remain above the lower band edge. Parameter: $u = 1.5$, $v = -5$, $g = 0.03$.

This has to be compared with the Feshbach scattering in homogeneous space according to equation (24) and has been presented already in figure 2. There, the resonance energy $E = \varepsilon_{\text{res}} + Q^2/4 > 0$ is on a simple parabola as a function of Q. If we tune the Feshbach resonance energy $\varepsilon_{\text{res}} < 0$, it either disappears completely or is always present.

5. Experimental considerations

Starting from a dilute Fermi gas, atoms can be loaded adiabatically into the lowest energy band of the lattice. For quasi-momenta not too close to the band edge, this requires that the Fermi energy remains clearly below the atomic recoil energy $\hbar\omega_r$, corresponding to $2\pi \times$

8.4 kHz and $2\pi \times 74$ kHz for the ^{40}K and ^{6}Li D2-lines respectively[4]. To ensure that the Feshbach resonance provides coupling only within a single-energy band, its width has to be sufficiently narrow, i.e. below a value of about $\hbar\omega_r/\Delta\mu$, where $\Delta\mu$ denotes the difference of the atomic and the molecular states magnetic moments respectively. For typical parameters, we arrive at a required width of the Feshbach resonance below 10–100 mG. We are aware that the investigation of such weak Feshbach resonances requires a high magnetic field stability. On the other hand, three-body losses, which for free space experiments are a mayor second experimental constraint in the study of narrow Feshbach resonances, are expected to be reduced in the presence of the lattice potential due to atom localization in the micropotentials.

For an experimental verification of the relative atomic momentum dependence of the Feshbach resonance, as indicated in figures 11 and 12, one could study such scattering resonances for a variable filling of the lowest energy band in the lattice. In this way, due to the Pauli exclusion principle, for an increased band filling different regions of the relative atomic quasi-momentum are subsequently filled up. The variation of the lineshape of the Feshbach resonance is determined by the collisional properties of atoms in the lattice. For example, if we take the situation of figure 11, for small atom filling the scattering resonance would disappear. The Feshbach resonance here could only be observed for a large atom filling.

6. Conclusions and outlook

We have considered Feshbach scattering of two Fermions in a one-dimensional optical lattice. Due to the reduction of translation invariance, the relative and centre-of-mass motion are coupled and we present the scattering theory in the crystal momentum basis. Within a single-band approximation, we have calculated numerically Feshbach resonances and demonstrate that the position of the Feshbach resonance depends selectively on the centre-of-mass momentum, due to the non-parabolic shape of the energy band. The simple resonance structure suggests that a semi-analytical calculation based on an effective-mass approximation should be applicable and is currently pursued.

In the present paper, we have only considered Feshbach resonances that are much weaker than the interband separation. Thus, we could limit the discussion to a single-energy band. Wider Feshbach resonances will involve the coupling of several bands. Going beyond the single-band approximations will provide interesting new physics as already advanced in [25] for the case of potential scattering. This will be examined, based on the present formulation, in a forthcoming publication.

Acknowledgments

We gratefully acknowledge financial support by the SFB/TRR 21 '*Control of quantum correlations in tailored matter*' funded by the Deutsche Forschungsgemeinschaft (DFG). MG and RW are also grateful for the hospitality of the Centro International de Ciencias A.C. (CICC) in Cuernavaca, Mexico.

References

[1] Slater J 1958 Interaction of waves in crystals *Rev. Mod. Phys.* **30** 197
[2] Callaway J 1991 *Quantum Theory of the Solid State* (New York: Academic)
[3] Batterman B and Cole H 1964 Dynamical diffraction of x rays by perfect crystals *Rev. Mod. Phys.* **36** 681

[4] Here $\hbar\omega_r = \hbar^2k^2/2m \equiv \varepsilon_r/2$ represents half the energy unit defined in (15).

[4] Cohen-Tannoudji C 1990 Atomic motion in laser light *Le Houches Lecture Notes, Course XXX (Fundamental Systems in Quantum Optics)* ed J Dalibard, J Raimond and J Zinn-Justin (Amsterdam: Elsevier)
[5] Taylor J 2000 *Scattering Theory* (New York: Dover)
[6] Weitz M, Cennini G, Ritt G and Geckeler C 2004 Optical multiphoton lattices *Phys. Rev.* A **70** 043414
[7] Jaksch D, Bruder C, Cirac J, Gardiner C and Zoller P 1998 Cold bosonic atoms in optical lattices *Phys. Rev. Lett.* **81** 3108
[8] Kollath C, Schollwöck U, von Delft J and Zwerger W 2004 Spatial correlations of trapped one-dimensional bosons in an optical lattice *Phys. Rev.* A **69** 31601
[9] Bloch I 2005 Ultracold quantum gases in optical lattices *Nature Phys.* **1** 23
[10] Morsch O and Oberthaler M 2006 Dynamics of Bose–Einstein condensates in optical lattices *Rev. Mod. Phys.* **78** 179
[11] Rigol M, Muramatsu A, Batrouni G and Scalettar R 2003 Local quantum criticality in confined fermions on optical lattices *Phys. Rev. Lett.* **91** 130403
[12] Rigol M and Muramatsu A 2004 Quantum Monte Carlo study of confined fermions in one-dimensional optical lattices *Phys. Rev.* A **69** 053612
[13] Köhl M, Moritz H, Stöferle Th, Günter K and Esslinger T 2005 Fermionic atoms in a three dimensional optical lattice: observing Fermi surfaces, dynamics, and interactions *Phys. Rev. Lett.* **94** 080403
[14] Orso G and Shlyapnikov G 2005 Superfluid Fermi gas in a 1d optical lattice *Phys. Rev. Lett.* **95** 260402
[15] Carr L and Holland M 2005 Quantum phase transitions in the Fermi–Bose Hubbard model *Phys. Rev.* A **72** 031604
[16] Ospelkaus C, Ospelkaus S, Humbert L, Ernst P, Sengstock K and Bongs K 2006 Ultracold heteronuclear molecules in a 3d optical lattice *Phys. Rev. Lett.* **97** 120402
[17] Dickerscheid D B and Stoof H T 2005 Feshbach molecules in a one-dimensional Fermi gas *Phys. Rev.* A **72** 053625
[18] Orso G, Pitaevskii L P, Stringari S and Wouters M 2005 Formation of molecules near a Feshbach resonance in a 1d optical lattice *Phys. Rev. Lett.* **95** 060402
[19] Stöferle Th, Moritz H, Günter K, Köhl M and Esslinger T 2006 Molecules of fermionic atoms in an optical lattice *Phys. Rev. Lett.* **96** 030401
[20] Winkler K, Thalhammer G, Lang F, Grimm R, Hecker-Denschlag J, Daley A J, Kantian A, Büchler H P and Zoller P 2006 Repulsively bound atom pairs in an optical lattice *Nature* **441** 853
[21] Wouters M and Orso G 2006 Two-body problem in periodic potentials *Phys. Rev.* A **73** 012707
[22] Grupp M, Nandi G, Walser R and Schleich W P 2006 Collective Feshbach scattering of a superfluid droplet from a mesoscopic two-component Bose–Einstein condensate *Phys. Rev.* A **73** 50701
[23] Adams E 1952 Motion of an electron in a perturbed electronic potential *Phys. Rev.* **85** 41
[24] Tiesinga E, Moerdijk A, Verhaar B and Stoof H 1992 Conditions for Bose–Einstein condensation in magnetically trapped atomic cesium *Phys. Rev.* A **46** 1167
[25] Diener R and Ho T 2006 Fermions in optical lattices swept across Feshbach resonances *Phys. Rev. Lett.* **96** 010402
[26] Regal C, Ticknor C, Bohn J and Jin D 2003 Creation of ultracold molecules from a Fermi gas of atoms *Nature* **424** 47
[27] Chin C, Bartenstein M, Altmeyer A, Riedl S, Jochim S, Hecker-Denschlag J and Grimm R 2004 Observation of the pairing gap in a strongly interacting Fermi gas *Science* **305** 1128
[28] Zwierlein M, Stan C, Schunck C, Raupach S, Kerman A and Ketterle W 2004 Condensation of pairs of fermionic atoms near a Feshbach resonance *Phys. Rev. Lett.* **92** 120403
[29] Holland M, Kokkelmans S J J M F, Chiofalo M and Walser R 2001 Resonance superfluidity in a quantum degenerate Fermi gas *Phys. Rev. Lett.* **87** 120406
[30] Kokkelmans S, Milstein J, Chiofalo M L, Walser R and Holland M 2002 Resonance superfluidity: renormalization of resonance scattering theory *Phys. Rev.* A **65** 053617
[31] Fano U 1961 Effects of configuration interaction on intensities and phase shifts *Phys. Rev.* **124** 1866
[32] Feshbach H 1958 A unified theory of nuclear reactions *Ann. Phys.* **5** 357
[33] Feshbach H 1962 A unified theory of nuclear reactions. II *Ann. Phys.* **19** 287
[34] Bilhorn D and Tobocman W 1961 Coupled square well model for elastic scattering *Phys. Rev.* **122** 1517
[35] Friedrich H 1990 *Theoretische Atomphysik* (Berlin: Springer)
[36] Kohn W 1959 Analytic properties of Bloch waves and Wannier functions *Phys. Rev.* **115** 809